

Mueller-Tang jets in next-to-leading BFKL*

DIMITRI COLFERAI

Department of Physics, University of Florence and INFN Florence

Received November 29, 2022

We provide first predictions for the cross section of Mueller-Tang jets at LHC. Our calculation is based on a factorization formula of BFKL type that represents exchanges of colour-singlet objects among the external particles. This formula resums to all perturbative orders a certain class of Feynman diagrams that are supposed to dominate the cross section in the Regge limit. Our explicit calculations at next-to-leading logarithmic order questions the validity of such factorization when an IR safe jet algorithm is used to reconstruct jets. We show the origin of such violation of factorization, and quantify its impact for LHC phenomenology.

1. Introduction

Mueller-Tang (MT) jets [1] are important for studying perturbative high-energy QCD and the Pomeron at hadron colliders. They are characterized by final states with at least two jets with comparable hard transverse momenta ($\mathbf{k}_{J1} \sim \mathbf{k}_{J2} \gg \Lambda_{QCD}$), well separated in rapidity $Y \equiv y_{J1} - y_{J2}$, and absence of emission in a given interval of pseudo-rapidity $\Delta\eta \lesssim Y$ in the central region (the so-called gap). A typical final state is depicted in fig. 1a.

The presence of the gap suggests that these events mainly occur when the momentum exchange between the forward and backward systems is due to a colour-singlet virtual state: a non-singlet exchange would be characterized most of the times by final state radiation deposited in the central region.

A large rapidity interval is possible because at LHC the center-of-mass (CM) energy is much larger than the jet transverse energy. In this case, the coefficients of the perturbative series are enhanced by powers of $Y \simeq \log(s/\mathbf{k}_j^2)$, and an all-order resummation of the leading terms $\sim (\alpha_s Y)^n$ is needed for a proper determination of the amplitude. The resummation of

* Presented at “Diffraction and Low- x 2022”, Corigliano Calabro (Italy), September 24-30, 2022.

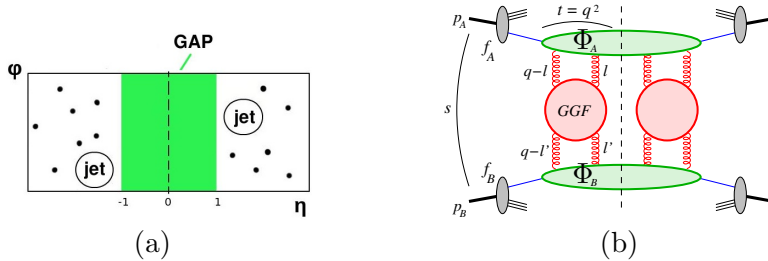


Fig. 1. (a) Sketch of Mueller-Tang jet event in the azimuth-rapidity plane. (b) Diagrammatic representation of the factorization formula for MT jets.

the logarithmically enhanced contribution to the cross section is embodied into the so-called BFKL gluon Green function (GGF) [2]. By squaring the partonic amplitude, the LL partonic cross-section is then given by the product of two GGFs (denoted by G), which embody the energy-dependence, and two *energy-independent* impact factors (IFs) denoted by Φ , that couple the gluons to the external particles. In the LL approximation the IFs are just a trivial product of coupling constants and colour factors. The ensuing factorization formula — involving also two PDFs describing the partonic content of hadrons — is thus (see fig. 1b)

$$\frac{d\sigma^{(LL)}}{dJ_1 dJ_2} \simeq \int d(x_1, x_2, \mathbf{l}_1, \mathbf{l}'_1, \mathbf{l}_2, \mathbf{l}'_2) f_A(x_1) \Phi_A(x_1, \mathbf{l}_1, \mathbf{l}_2; J_1) G(x_1 x_2 s, \mathbf{l}_1, \mathbf{l}_2) \times G(x_1 x_2 s, \mathbf{l}'_1, \mathbf{l}'_2) \Phi_B(x_2, \mathbf{l}'_1, \mathbf{l}'_2; J_2) f_B(x_2). \quad (1)$$

Here $J = (y_J, \mathbf{k}_J)$ represents the set of jet variables.

The importance of considering such BFKL contributions to the cross section has been emphasized since the first analysis by CMS. However the LL approximation is unable to describe data, even by adding next-to-leading logarithmic (NLL) contributions to the GGF.

2. Impact factor in next-to-leading logarithmic approximation

It appears thus compelling to provide a full NLL description of MT jets. This requires the calculation of singlet non-forward GGF and impact factors in NLL approximation.

The NLL BFKL GGF is known in the non-forward case [3], but due to its complexity, only the forward version [4, 5], has been used in order to estimate the contribution of NL logarithmic terms to the cross section [6].

The calculation of NL IF for MT jets was performed [7] using Lipatov's effective action, and has been confirmed by our independent calculation.

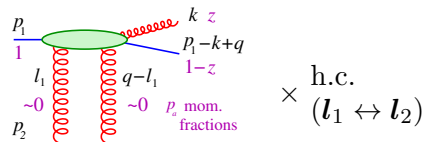


Fig. 2. Kinematics of the calculation of the NL impact factor. Black symbols denote 4-vectors, while purple ones denote longitudinal momentum fraction.

This is the structure of the result in the case of incoming quark:

$$\Phi(\mathbf{l}_1, \mathbf{l}_2, \mathbf{q}) = \frac{\alpha_s^3}{2\pi(N_c^2 - 1)} \int_0^1 dz \int d\mathbf{k} S_J(\mathbf{k}, \mathbf{q}, z) C_F \frac{1 + (1-z)^2}{z} \times \left\{ C_F^2 \frac{z^2 \mathbf{q}^2}{\mathbf{k}^2 (\mathbf{k} - z\mathbf{q})^2} + C_F C_A f_1(\mathbf{l}_{1,2}, \mathbf{k}, \mathbf{q}, z) + C_A^2 f_2(\mathbf{l}_{1,2}, \mathbf{k}, \mathbf{q}) \right\}.$$

It is important to understand the kinematics of the process (see fig. 2): after the “upper” incoming quark interacts with the two gluons in colour-singlet, a quark and a gluon can be found in the forward hemisphere of the final state; the “lower” parton p_2 remains intact and is just slightly deflected in the backward hemisphere.

We denote with k the outgoing gluon momentum, with \mathbf{k} its transverse momentum and with z its longitudinal momentum fraction with respect to the parent quark, q is the overall t -channel transferred momentum, \mathbf{k} and z are integration variables. Virtual contributions are contained as delta-function contributions at $z = 0$ and $\mathbf{k} = 0$.

We can see the quark-to-gluon splitting function P_{gq} as overall factor, and then three terms with different colour structures. The integration in the phase space of the gluon and quark final state has to be restricted by an IR-safe jet algorithm S_J , such as the k_{\perp} -algorithm.

3. Violation of BFKL factorization

In the diffractive process we are considering, one quark moves in the backward direction and is identified with the backward jet. The other two partons, whose distance in azimuth-rapidity is $\Delta\Omega = \sqrt{\Delta\phi^2 + \Delta y^2}$, are emitted in the forward hemisphere, so as to produce at least one jet. There are three possibilities: (i) $\Omega < R$ corresponding to a composite jet; (ii) $\Omega > R$ where the *gluon is the jet* and the quark is outside the jet cone; (iii) $\Omega > R$ where the *quark is the jet* and the gluon is outside the jet cone. In the last configuration there is a problem due to the dz/z integration of the

$C_A^2 f_2$ term. In fact, when the quark is the jet, the gluon can become soft and its phase-space integration is essentially unconstrained.

The limit $z \rightarrow 0$ at fixed \mathbf{k} corresponds to find the gluon in the central (and backward) region, where the emission probability of the gluon turns out to be flat in rapidity, and formally the z (or y_g) integration diverges.

If we believe the above transition probability to be reliable at least in the forward hemisphere ($y_g > 0$), the longitudinal integration yields a $\log s$. But a $\log s$ in the IF is not acceptable, being against the spirit of BFKL factorization where all the energy-dependence is embodied in the GGFs.

This is somewhat unexpected, because one would have argued that gluon emission in the central region should be dynamical suppressed, due to the singlet exchange in the t -channel. In order to find the origin of such logarithmic contributions in the IF, let us consider a pair of diagrams contributing to the $C_A^2 f_2$ term and drawn in fig. 3. It is clear that, if the two t -channel (vertical) gluons emitted by the lower quark are in a colour-singlet state, by colour conservation the (one or two) upper gluons cannot be in such a state, since a (coloured) gluon is emitted in the final state.

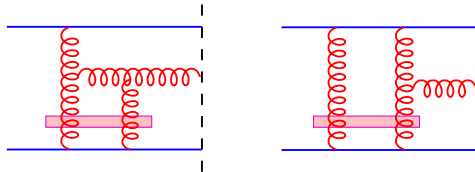


Fig. 3. Diagrams that involve a non-singlet emission “above” the emitted gluon.

Therefore, the impact factors for MT jets involve logarithmic terms that are not compatible with the original requirement of the BFKL factorization formula. We therefore claim that MT jets are not describable by the naive factorization formula originally proposed. One can easily estimate that the logarithmic contribution to the impact factor is of order $\Phi_{log} \sim C_A^2 \frac{E_{th}^2}{\mathbf{k}_J^2} \log \frac{s}{\mathbf{k}_J^2}$, where $E_{th} \lesssim 1$ GeV is the threshold energy below which particles cannot be detected. Note that this term is regular for $E_{th} \rightarrow 0$, actually it vanishes, at variance with the $\mathcal{O}(C_F^2)$ term in the IF which diverges in the same limit. When evaluated with the values of energies and momenta of typical processes analysed at LHC, this term turns out to be small, of order 6% or less with respect to other terms.

Although not really needed from a quantitative point of view at the moment, one could envisage to resum such logs in the same BFKL spirit, i.e. by considering diagrams where an arbitrary number of soft (below threshold) gluons are emitted in the gap (without being detected).

4. Results

In this section we show our results for the differential cross section as function of the rapidity distance Y between the jets, adopting the CMS setup for data selection: $\sqrt{s} = 14$ TeV, $E_J \geq 40$ GeV, $1.5 \leq |y_J| \leq 5$, $y_{\text{gap}} \in [-1, 1]$, $E_{\text{th}} = 1.0$ GeV. In fig. 4.a we compare predictions in 3 approximations: pure LL (red), leading IFs and NLL GGF (orange), full NLL (blue). The NL corrections to IFs provide a slightly steeper decrease of the cross section.

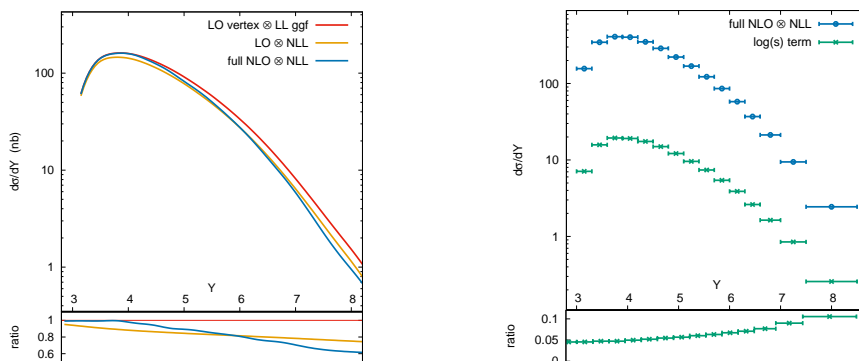


Fig. 4. (a) LL and NLL cross sections; (b) impact of $\log s$ term.

In fig. 4.b we compare the full NL cross section (blue) with the contribution of the logarithmic term responsible of the violation of factorization (green), which turns out to be rather small $\sim 6\%$, within the theoretical uncertainties stemming from energy-scale and renormalization-scale variations.

Fig. 5.a shows the uncertainty bands for variations of the energy scale $s_0 \simeq E_{J1}E_{J2}$ by a factor of two. The red band is for the LL prediction, the dashed blue lines for the full NL cross section. The energy scale dependence is reduced at moderate Y , but it increases at large Y .

Fig. 5.b shows the uncertainty bands for variations of the running-coupling scale $\mu_R \simeq E_{J1} + E_{J2}$ by a factor of two. The red band is for the LL prediction, the dashed blue lines for the full NL cross section. The renormalization scale dependence is still large in NLA, and suggests to adopt a method like BLM or PMS for its fixing. The minimum sensitivity (stability w.r.t. variation of μ_R) is reached for a value of μ_R which is four times the natural value.

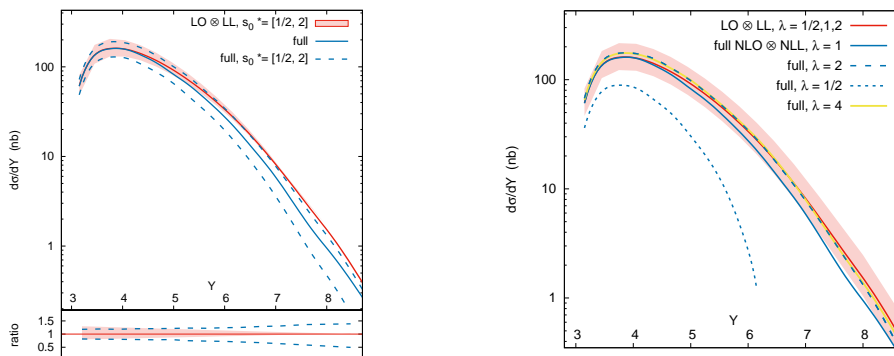


Fig. 5. Variation of cross section w.r.t. energy and renormalisation scale changes.

5. Conclusions

We have shown that, for MT jets, there is violation of the standard BFKL factorization at NLL level, since the IFs present logarithmically enhanced energy-dependent contributions. However such terms are rather small, below few % for current measurements of Mueller-Tang jets at LHC.

The full NL prediction is somewhat smaller and with a steeper decrease w.r.t. Y than the LL one. The relative theoretical uncertainty is about 30%. In particular, the dependence on the renormalisation scale suggests a value of μ_R about 4 times larger than the natural scale.



This project has received funding from the European Union's Horizon 2020 research and innovation programme under grant agreement No 824093.

REFERENCES

- [1] A. H. Mueller and W. K. Tang, Phys. Lett. B **284** (1992), 123-126.
- [2] L. N. Lipatov, Sov. J. Nucl. Phys. **23** (1976), 338-345;
E. A. Kuraev, L. N. Lipatov and V. S. Fadin, [Zh.Eksp.Teor.Fiz.**72** (1977) 377];
I. I. Balitsky and L. N. Lipatov, Sov. J. Nucl. Phys. **28** (1978) 822.
- [3] V. S. Fadin and R. Fiore, Phys. Rev. D **72** (2005), 014018.
- [4] V.S. Fadin and L.N. Lipatov, Phys. Lett. **B 429** (1998) 127.
- [5] G. Camici and M. Ciafaloni, Phys. Lett. **B 430** (1998) 349.
- [6] O. Kepka, C. Marquet and C. Royon, Phys. Rev. D **83** (2011), 034036.
- [7] M. Hentschinski, J. D. . Martínez, B. Murdaca and A. Sabio Vera, Nucl. Phys. B **887** (2014), 309-337; Nucl. Phys. B **889** (2014), 549-579.